## The long non-coding RNA *Cancer Susceptibility 15* (*CASC15*) is induced by isocitrate dehydrogenase (IDH) mutations and maintains an immature phenotype in adult acute myeloid leukemia

We and others recently showed that coordinated expression of long non-coding (lnc)RNA is essential for myeloid differentiation and that, in turn, deregulation of lncRNA contributes to the pathogenesis of acute myeloid leukemia (AML).[1] To better understand the relationship between lncRNA that control granulopoiesis and the block of differentiation in AML blasts, we sequenced stranded, non-poly-A-enriched cDNA libraries that were prepared from healthy human donor bone marrow (deposited under GEO accession number #GSE98946). Within this dataset, expression of the lncRNA *Cancer Susceptibility 15* (*CASC15*) was significantly inversely correlated with myeloid differentiation and highly enriched in myeloblasts,[1] which suggests a role in maintaining stem cell features such as an immature phenotype and/or self-renewal. Due to the reported proto-oncogenic role of *CASC15* in childhood AML,[2] we further explored *CASC15* in the context of adult AML, especially in patients with mutated *isocitrate dehydrogenase* (*IDH*).

**A** Apoptosis [GM-CSF depletion]

| | Control [%] | *CASC15* -KO [%] |
|---|---|---|
| unstained | 70.4 | 71.1 |
| Annexin-V+ | 11.2 | 8.0 |
| Annexin/Sytox-double+ | 10.4 | 8.6 |
| Sytox+ | 8.0 | 12.3 |

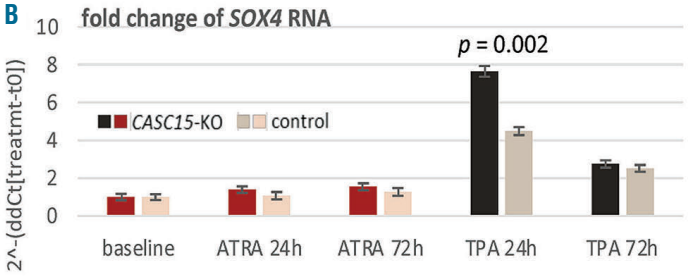


**C** myeloid surface marker profile

| | Control [%] | *CASC15* -KO [%] |
|---|---|---|
| CD11b | 85.5 | 92.4 |
| CD11c | 15.8 | 20.1 |
| CD13 | 3.2 | 7.3 |
| CD14 | 0.4 | 1 |
| CD15 | 0.2 | 0.3 |

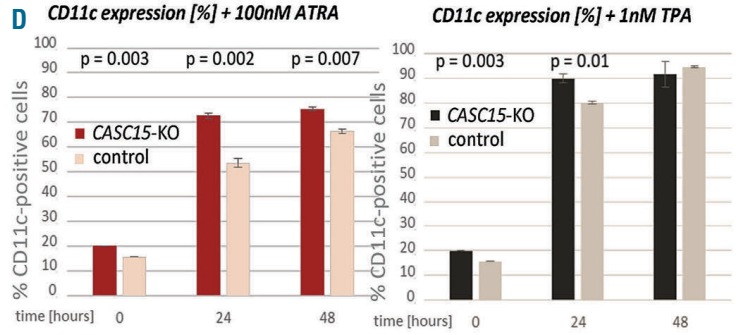


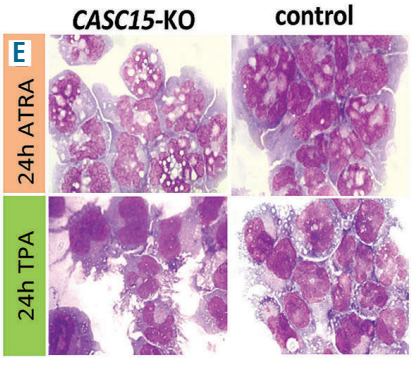


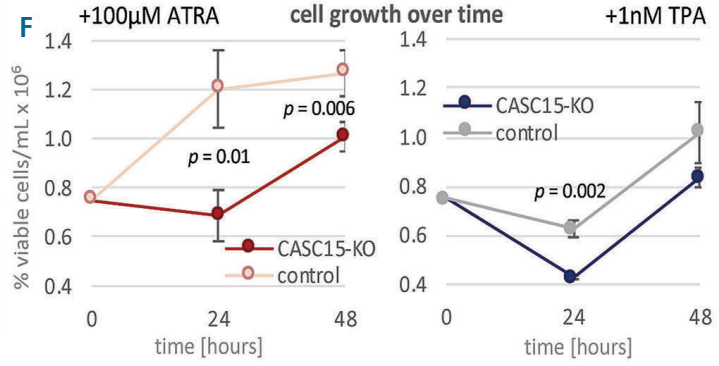


**Figure 1 *CASC15*-KO promotes the differentiation of acute myeloid leukemia cells.** (A) Apoptosis in *CASC15*-KO and empty vector-transduced (control) OCI-AML5 cell lines after 24 h of depletion of granulocyte-macrophage colony-stimulating factor (annexin-FITC/Sytox blue flow cytometry). (B) Expression of SOX4 during *in vitro* differentiation of *CASC15*-KO and control OCI-AML5 cell lines. All cells were treated with 0.1 µM all-*trans* retinoic acid (ATRA) and 1 nM 12-O-tetradecanoylphorbol-13-acetate (TPA) over 72 h in three independent experiments. Total RNA was extracted before, after 24 h and after 72 h of treatment, DNase-digested and transcribed to cDNA. A quantitative real-time polymerase chain reaction (qRT-PCR) was performed using SYBR green chemistry with subsequent melting curve analysis in technical triplicates. The $2^{-ddCt}$ was calculated relative to the pre-determined housekeeping gene encoding succinate dehydrogenase complex subunit C (*SDHC*). (C) Baseline expression of the monocyte/macrophage markers CD11b (integrin subunit alpha M, ITGAM), CD11c (integrin subunit alpha X, ITGAX), and CD14, the granulocyte marker CD15 (fucosyltransferase 4, FUT4), and the general myeloid marker CD13 (aminopeptidase N, APN) in *CASC15*-KO and control cells. The percentages of positive cells, quantified by flow cytometry after 72 h, are shown. (D-F) Growth rate and CD11c myeloid cell surface marker expression of *CASC15* and control cell lines during drug-induced *in vitro* differentiation (D) Cells ($0.75x10^6$/mL) were seeded and treated with 0.1 µM ATRA, 1 nM TPA or 0.1 µM vehicle control (dimethylsulfoxide) for 48 h in three independent experiments. CD11c was stained and quantified before (baseline/t0), after 24 h and after 48 h of treatment on 10,000 cells per sample by flow cytometry. (E) Cellular morphology was assessed in cytospins stained with May-Grünwald/Giemsa. (F) Number of trypan blue-negative cells 24 h and 48 h after drug treatment. *(Figure continued on the next page)*

*Figure 1 continued from the previous page)*

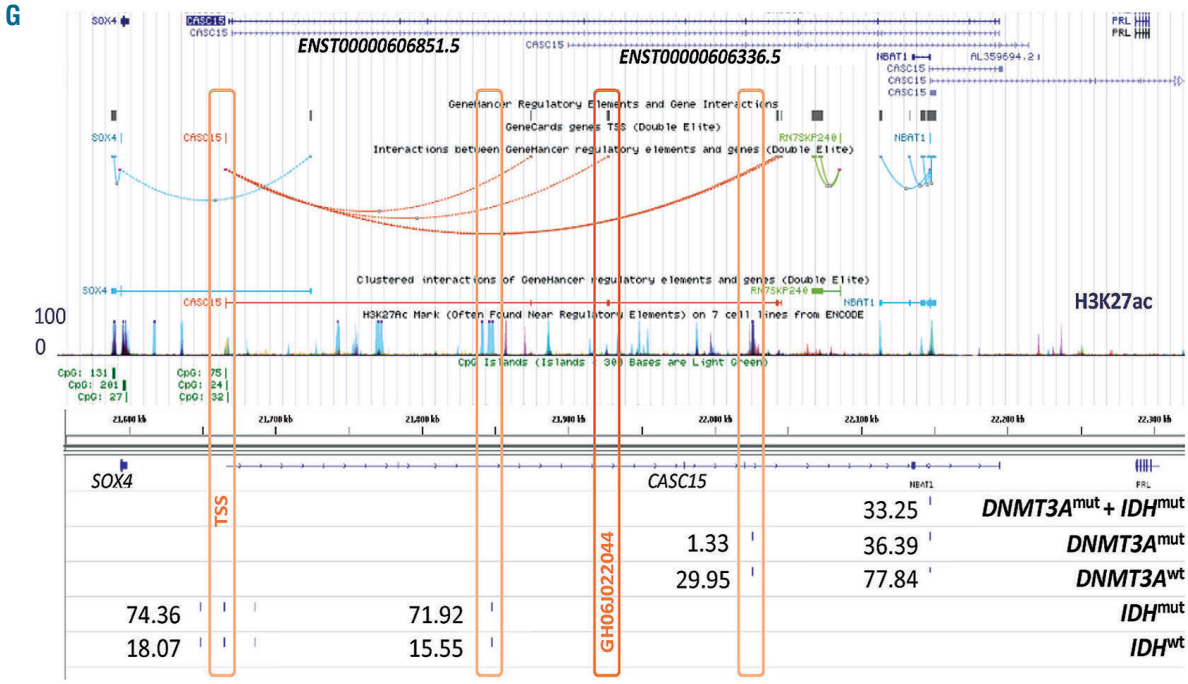


**Figure 1 (continued).** (G) The *SOX4, CASC15*, and *NBAT1* genomic loci displayed in the University of California, Sant Cruz (UCSC) genome browser with subordinated tracks showing currently annotated isoforms (GENCODE v29), GeneHancer-listed regulatory elements, layered H3K27 acetylation (ENCODE), 5'-C-phosphate-G-3' (CpG) sites, and percent methylation determined *via* enhanced reduced representation bisulfite sequencing (ERRBS) in *IDH*-mutant (n=9), *DNMT3A*-mutant (n=16), and *IDH/DNMT3A* double-mutant (n=11) AML patients relative to normal controls. The ERRBS data were produced and normalized by Glass *et al.*[8] (Gene Expression Omnibus identiy: GSE86952). *P*-values were calculated using a paired Welch two sample *t*-test after testing for unequal variance.

To assess the role of *CASC15* in human AML cells, we genetically deleted the promoter and transcription start site of *CASC15* in the human OCI-AML-5 cell line *via* a CRISPR/Cas9 approach (*CASC15*-KO). In brief, OCI-AML-5 cells were transduced with Cas9-ORF-carrying a DHC013 vector and selected with 5 μg/mL blasticidin. Cas9 expression was confirmed by western blotting. Single guide (sg)RNA were designed using CCTop (*https://crispr.cos.uni-heidelberg.de/*): T1: 5'-CACCGATG-GATTACAATTTGATCGC-3'fw, 5'-AAACGCGAT-CAAATTGTAATCCATC-3'rev; T2: 5'-CACCgATTAATTAAAGTTAGCTTCC-3'fw, 5'-AAACGGAAGCTAACTTTAATTAATC-3'rev. Each sgRNA pair was cloned into either *pL40C-CRISPR.EFS.PAC* or *pL-CRISPR.EFS.tRFP*, respectively (kindly provided by Dirk Heckl), each with the Cas9-ORF removed. Cells ($1x10^6$/mL) were spin-infected with an equimolar mix of virus-containing medium + 10 mg/mL polybrene. Single-cell clones were sorted, expanded in 1 μg/mL puromycin, and sent for Sanger sequencing. Lack of *CASC15* expression was confirmed in heterozygous knock-out (KO) and control cell lines *via* polymerase chain reaction (PCR) (PlatinumTaq, ThermoFisher Scientific) and quantitative real-time PCR (qRT-PCR) (TBgreen, TaKaRa, Japan) using the following primer sets: *CASC15* exon1: 5'-GGGTATCTCCCTCTCG-CAAC-3'fw, 5'-CGTTCGGACACTTTTTCCCG-3'rev; *CASC15* exon2: 5'-TGACCTCCTTCATTCTGCGTT-3'fw, 5'-GGGTATAAGCCCCAGACCAA-3'rev. Loss of *CASC15* did not sustainably affect apoptosis or *SOX4* RNA levels in these cells (Figure 1A, B), as was previously reported for *CASC15*-KO in a *RUNX1*-rearranged AML background,[2] but increased the expression of myeloid surface markers (Figure 1C). To induce differentiation, we treated $0.75x10^6$ cells with 1 nM 12-O-tetradecanoylphorbol-13-acetate (TPA) or 100 nM all-*trans* retinoic acid (ATRA) (Sigma-Aldrich) and assessed the level of differentiation by flow cytometry using α-CD11b-APC (#17-0118-41, clone ICRF44, eBioscience, San Diego, CA, USA), α-CD11c-APC (#17-0116-42, clone 3.9, ThermoFisher Scientific, USA), α-CD13-FITC (#ab52461, clone WM15, abcam, Cambridge, UK), and α-CD14-APC (#17-0149-42, clone 61D3, eBioscience), α-CD15-FITC (#555401, lot 13878, Becton Dickinson, San Jose, CA, USA) antibodies.

In response to TPA and ATRA, *CASC15*-KO cells showed enhanced myeloid differentiation and reduced proliferation compared to the empty vector control cells (Figure 1D-F), suggesting that the presence of *CASC15* contributes to the block of differentiation in human AML cells.

The highly complex genomic structure of the *CASC15* locus pointed towards an equally complex transcriptional regulation and post-transcriptional processing of this (lnc)RNA (Figure 1G). Interrogating the entire transcription factor and co-factor footprinting data generated for the ENCODE project in K562 cells,[4] we observed that the strongest binding intensities at the *CASC15* site were for the erythroid differentiation factor TAL-1, the proto-oncogenic proteins JunD and c-MYC/MAZ, the co-acti-

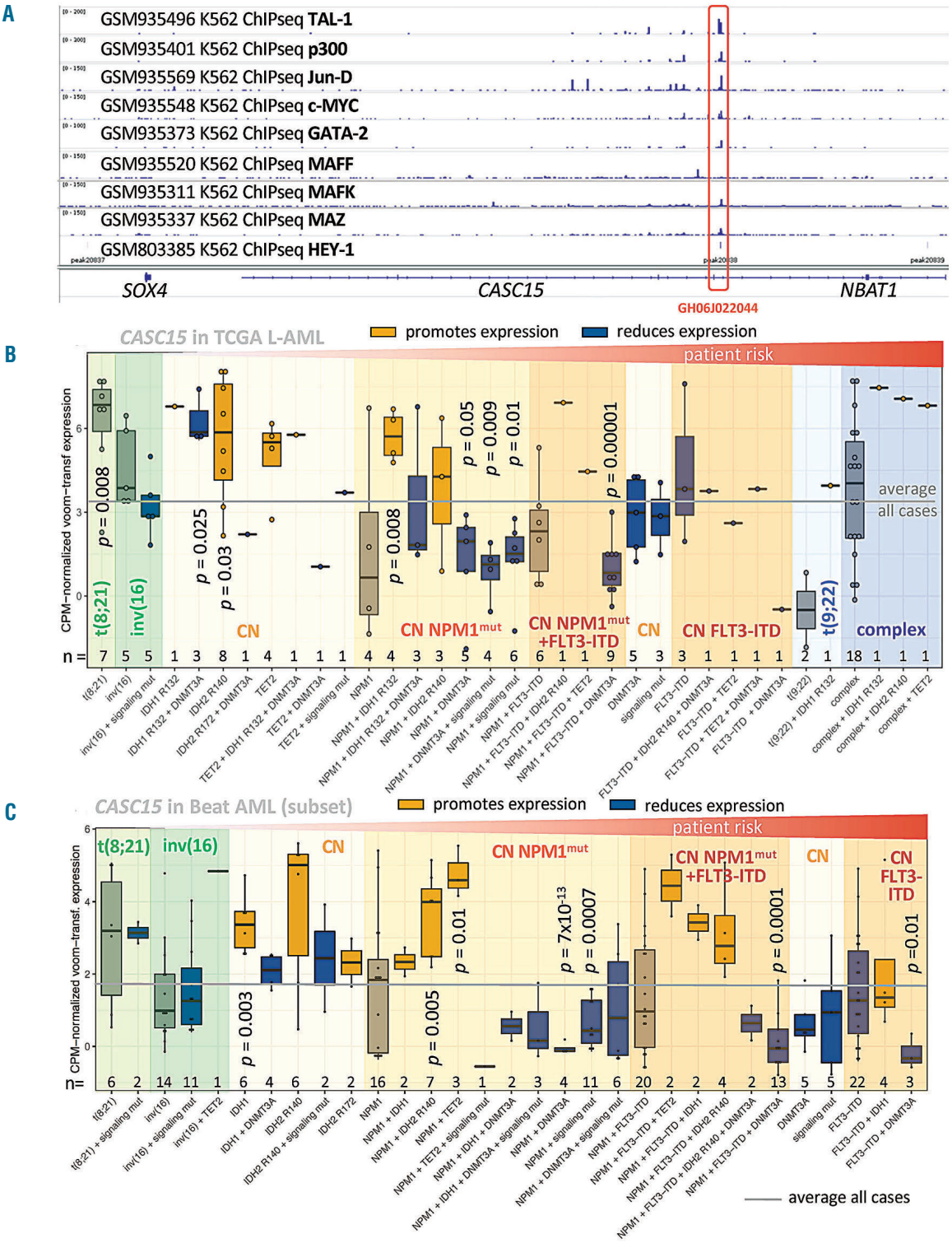


**Figure 2. *CASC15* is bound by hematopoiesis-regulating transcription factors and its expression reflects the patients' *IDH* mutational status.** (A) Chromatin immunoprecipitation sequencing (ChIPseq) data showing the location and intensity of transcription factor binding at the *CASC15* genomic site, mapped to the hg19 human genome release. Data were produced and processed within the ENCODE project[6] (Gene Expression Omnibus accession identities: GSE31477 and GSE32465). (B) Expression of *CASC15* in a subset of the TCGA L-AML cohort[12] (n=122), excluding *MLL*-rearranged, t(15;17), and aneuploid cases, subdivided according to recurrent cytogenetic and molecular abnormalities. RNA-sequencing data were TMM-normalized and $\log_2$-counts per million-transformed (*limma*).[13] *P*-values were calculated comparing the individual groups to all cases using the Welch two-sample *t*-test and adjusted for multiple hypothesis testing. (C) Expression of *CASC15* in a subset of t(8;21), inv(16), and cytogenetically normal patients with acute myeloid leukemia (AML) from the Beat AML Master Trial[20] subdivided according to the recurrent cytogenetic and molecular abnormalities of interest. RNA sequencing data were TMM-normalized and $\log_2$-counts per million-transformed (*limma*).[13] *P*-values were calculated comparing the individual groups to all cases using the Welch two-sample *t*-test and adjusted for multiple hypothesis testing.

vator p300, as well as for HEY-1, GATA-2, and members of the MAFF/BZIP family (Figure 2A). These transcription factors predominantly occupy the annotated *CASC15* enhancer *GH06J022044*, which is located in intron 7 (GeneHancer v2, Jan 2019) (Figure 1G), share a strong enrichment for the basic helix-loop-helix motif, and are associated with transcriptional control in non-committed myeloid progenitors.[5] This suggests that *CASC15* is regulated by myeloid transcription factors, supporting our findings in human myeloblasts and AML cells.

In four independent transcriptome datasets (including the Beat AML and TCGA LAML cohorts as well as GEO datasets #GSE6891 and #GSE104099, for a total of 1,145 patients), we observed the highest *CASC15* expression in AML patients with t(8;21) and in cytogenetically normal AML patients harboring *IDH* or *TET2* mutations (shown

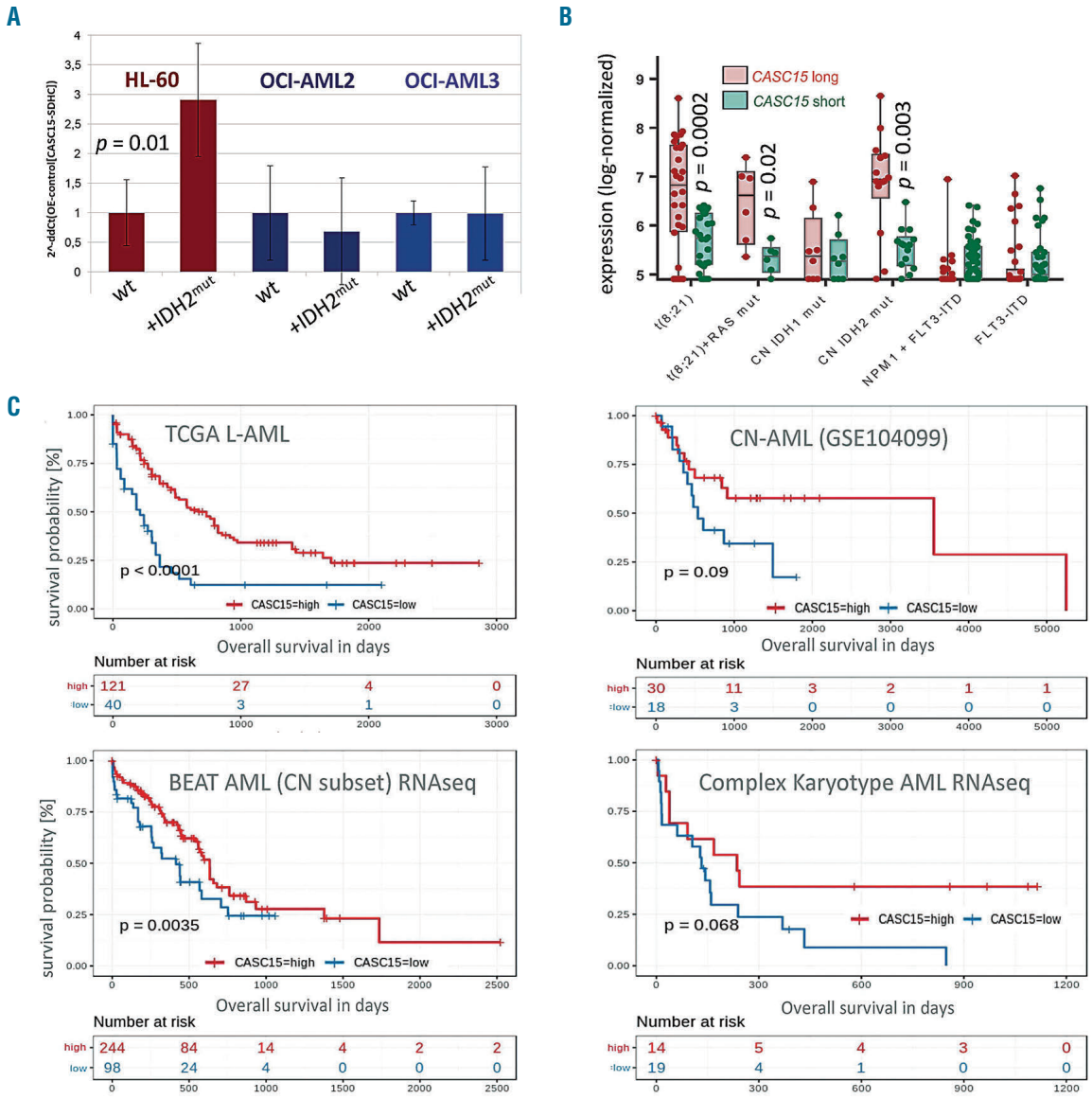


**Figure 3. Expression of *CASC15* is associated with patients' survival, is induced by *IDH* mutations and antagonized by mutant *DNMT3A*.** (A) Expression of *CASC15* in *IDH2*$^{R172K}$ cDNA-overexpressing *DNMT3A* wild-type (HL-60) and *DNMT3A*-mutant (OCI-AML2 and OCI-AML3) cell lines. Lentivirus-production and infection were performed in two independent experiments each and confirmed by flow cytometry. Total RNA was extracted, DNase-digested and transcribed to cDNA. A real-time quantitative polymerase chain reaction was performed using SYBR green chemistry with subsequent melting curve analysis in technical triplicates. The $2^{-ddCt}$ was calculated relative to the pre-determined housekeeping gene *SDHC*. (B) Expression of two *CASC15* transcript variants in bone marrow from patients with acute myeloid leukemia (AML), subdivided according to recurrent cytogenetic and molecular abnormalities of interest. *CASC15* long (red) shows log-normalized microarray data for probe 241047_at, which detects a short *CASC15* transcript isoform (*ENST00000606336.5*). *CASC15* short (green) shows log-normalized microarray data for probe 229280_s_at, detecting the longest *CASC15* transcript isoform including all currently annotated exons (*ENST00000606851.5*). Data were produced and normalized by Verhaak *et al.*[14] [Gene Expression Omnibus (GEO) accession identity: GSE6891]. *P*-values were calculated using a paired Welch two-sample *t*-test with 95% confidence and adjusted for multiple hypothesis testing. (C) Graphical representation of Kaplan-Meier estimates for the anti-differentiation transcript *CASC15* calculated in three publicly available and one in-house generated (CN-AML) cohort of adult AML patients. The patients in each cohort were dichotomized into those with *CASC15 high* (red) and *low* (blue) expression using maximally selected rank statistics.[15] Right-censored Kaplan-Meier estimates for overall survival were calculated using the R *survival* package with standard parameters. *P*-values were calculated using the log-rank test. *(Figure continued on the next page)*

*Figure 3 continued from the previous page)*

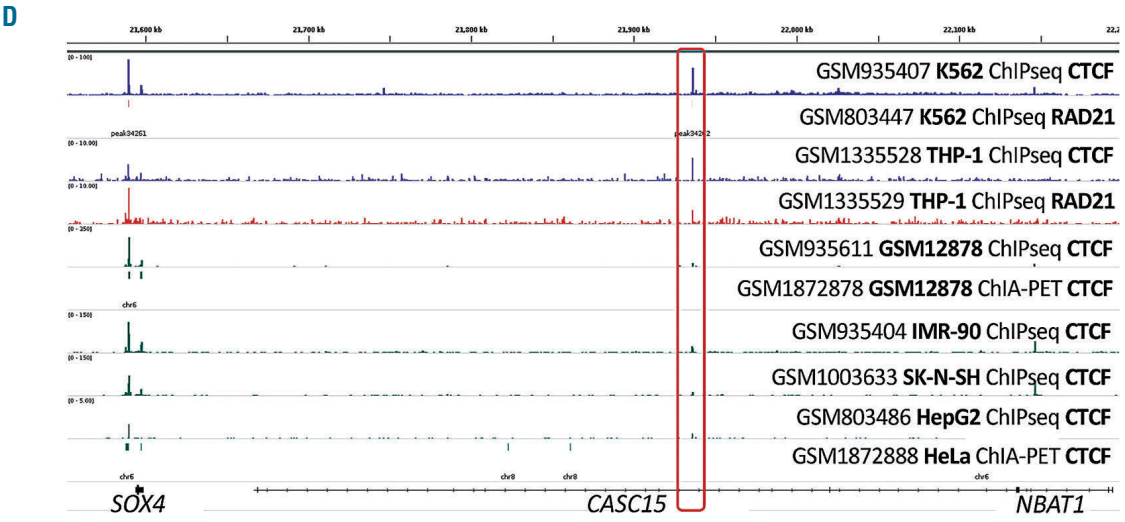


**Figure 3 (continued).** (D) AML cells possess a potential CTCF:RAD21-marked site that is not present in lymphoid and epithelial cells. CTCF-mapped chromatin interaction analysis by paired-end tag sequencing data were generated in GM12878 and HeLa cells by Tang *et al*. (GEO accession identity: GSE72816); chromatin immunoprecipitation sequencing (ChIPseq) data for CTCF and Rad21 in the THP-1 AML cell line were generated and analyzed by Rousseau *et al*. (GEO accession identity: GSE55407); ChIPseq data for CTCF and Rad21 in K562 cells were generated within the ENCODE project (GEO accession identity: GSE55407).[4]

for the 2 largest cohorts in Figure 2B, C). Mutations in *IDH1/2* and *TET2* represent early, almost mutually exclusive events in AML patients and are associated with a hypermethylation genotype as both mutations eventually reduce the cytosine demethylation activity of TET2.[6] In contrast, most *DNMT3A* mutations are thought to result in genome-wide CpG hypomethylation by formation of non-functional mutant:wild-type DNMT3A heterodimeric complexes.[7] *IDH* and *DNMT3A* mutations frequently co-occur in AML and genomes of *IDH/DNMT3A* double-mutant patients were found to exhibit an epigenetic antagonism, in which CpG that are affected by either mutation alone are no longer affected.[8] Interestingly, we observed strong downregulation of *CASC15* in patients carrying mutant *DNMT3A* or signaling-activating mutations (*FLT3, NRAS, KRAS, PTPN11*) (Figure 2B, C). We confirmed this by engineered overexpression of $IDH2^{R172K}$ mutant cDNA in human $DNMT3A^{wild\text{-}type}$ (HL-60) and $DNMT3A^{mutant}$ (OCI-AML2/3) AML cell lines. The $IDH2^{R172K}$-mutation was introduced into human $IDH2^{wild\text{-}type}$ cDNA *via* PCR (pEX-C0462-M02-50, Genecopoeia), cloned into a third-generation "self-inactivating" vector (kindly provided by Tobias Mätzig), and confirmed by Sanger sequencing. Lentiviral production and transduction were performed as previously described.[3] Whereas *CASC15* levels did not change in $DNMTA^{R635W}$ OCI-AML2 and $DNMTA^{R882C}$ OCI-AML3 cells, *CASC15* was significantly upregulated ($P$=0.01) in $DNMT3A^{wild\text{-}type}$ HL-60 cells in response to ectopic expression of mutant *IDH2* (Figure 3A).

A more detailed analysis of *CASC15* expression in subgroups of AML patients with different cytogenetic and molecular features revealed a generally balanced expression of two different *CASC15* isoforms: a short 7-exon (*ENST00000606336.5*) and a long *CASC15* transcript containing all 12 annotated exons (*ENST00000606851.5*) (Figure 1G). However, in $IDH2^{mutant}$ as well as in t(8;21) patients, in whom *CASC15* expression is highest, we detected a significantly ($P$<0.003) enriched expression of its long isoform (Figure 3B). This isoform switch was not observed in groups of patients with low *CASC15* expression, such as cytogenetically normal AML with *FLT3*-ITD (Figure 2B). This novel observation suggests differential or aberrant splicing in these subgroups of patients, with as of yet unknown cause or functional relevance.

In line with the elevated expression of *CASC15* in lower-risk cytogenetic and molecular AML subtypes, we found that high *CASC15* RNA expression was associated with improved overall survival in four independent adult AML datasets (n=584 patients) (Figure 3C).

Although we found CpG methylation to be generally increased in $IDH^{mut}$ and decreased in $DNMT3A^{mut}$ AML patients at the *CASC15* transcription start site and gene body (Figure 1G), the finding that *CASC15* is highly expressed in hypermethylated ($IDH^{mut}$ and $TET2^{mut}$) and less expressed in patients with hypomethylated genotypes ($DNMT3A^{mut}$ and $NPM1^{mut}$) suggests that these methylation changes do not directly affect *CASC15* transcription. The molecular consequences of *IDH* and *DNMT3A* mutations are not limited to epigenetic changes but also affect cellular metabolism and disturb DNA damage responses,[9,10] which is thought to promote genomic instability and to account for the high number of co-mutations observed in *IDH*- and *DNMT3A*-mutant leukemias. In comparison to the high *CASC15* levels in $IDH2^{R140}$ AML patients, we found that *CASC15* expression was often lower in $IDH1^{R132}$ and $IDH2^{R172}$ patients (Figure 2B, C), which underlines the presence of different transcriptional landscapes in each mutational entity[10] and suggests that the R140 and R172 mutations affect the cooperation of IDH2 with different interaction partners.

Finally, we also observed that the *CASC15* genomic site possesses a potential topologically-associating domain boundary in THP-1 and K562 myeloid leukemia cells, which is located between two *CASC15* enhancers

and is not present in non-myeloid cell lines (Figure 3D). Aberrant methylation at this CTCF-insulator in response to methylation-affecting mutations could be a plausible mechanism responsible for the counterintuitive expression of *CASC15* in hypo- *versus* hyper-methylated AML, as had already been shown in *IDH*-mutant gliomas,[11] and could potentially affect regional splicing.

In summary, we report that the survival-associated lncRNA *CASC15* acts as a proto-oncogene in AML cells, in which it affects proliferation and differentiation. We further found that its expression is indirectly linked to DNA methylation-affecting mutations and succumbs to splicing, potentially through a mechanism that involves an intragenic lineage-specific CTCF site. These novel insights warrant further investigation, especially in the context of treatment response to IDH inhibitors.

*Sarah Grasedieck,[1] Christoph Ruess,[1] Kathrin Krowiorz,[1] Susanne Lux,[1] Nicole Pochert,[1] Adrian Schwarzer,[2] Jan-Henning Klusmann,[2,3] Mojca Jongen-Lavrencic,[4] Tobias Herold,[5,6] Lars Bullinger,[7] Jonathan R. Pollack,[8] Arefeh Rouhi[1,9#] and Florian Kuchenbauer[1,9#]*

*[#]AR and FK contributed equally to this work as co-senior authors.*

*[1]Ulm University Hospital, Department of Internal Medicine III, Ulm, Germany; [2]Medizinische Hochschule Hannover (MHH), Hannover, Germany; [3]Universitätsklinik und Poliklinik für Pädiatrie I, Halle (Saale), Germany; [4]Erasmus University MC, Department of Hematology, Rotterdam, the Netherlands; [5]Department of Medicine III, University Hospital, LMU Munich, Munich, Germany; [6]Research Unit Apoptosis in Hematopoietic Stem Cells, Helmholtz Zentrum München, German Center for Environmental Health (HGMU), Munich, Germany; [7]Charité - Universitätsmedizin Berlin, Berlin, Germany; [8]Stanford University School of Medicine, Department of Pathology, Stanford, CA, USA and [9]Terry Fox Laboratory, BC Cancer Agency, Vancouver, British Columbia, Canada*

*Acknowledgments: the authors would like to thank Professor Hans-Jörg Fehling (Ulm University) for providing the IDH2$^{R172K}$ over-expression construct.*

*Correspondence:*

*FLORIAN KUCHENBAUER - fkuchenbauer@bccrc.ca*

*doi:10.3324/haematol.2019.235291*

## References

1. Schwarzer A, Emmrich S, Schmidt F, et al. The non-coding RNA landscape of human hematopoiesis and leukemia. Nat Commun. 2017;8(1):218.
2. Fernando TR, Contreras JR, Zampini M, et al. The lncRNA CASC15 regulates SOX4 expression in RUNX1-rearranged acute leukemia. Mol Cancer. 2017;16(1):126.
3. Azoitei N, Diepold K, Brunner C, et al. HSP90 supports tumor growth and angiogenesis through PRKD2 protein stabilization. Cancer Res. 2014;74(23):7125-7136.
4. Gertz J, Savic D, Varley KE, et al. Distinct properties of cell-type-specific and shared transcription factor binding sites. Mol Cell. 2013; 52(1):25-36.
5. Valledor AF, Borràs FE, Cellell-Young M, Celada A. Transcription factors that regulate monocyte/macrophage differentiation. J Leukoc Biol. 1998;63(4):405-417.
6. Figueroa ME, Abdel-Whab O, Lu C, et al. Leukemic IDH1 and IDH2 mutations result in a hypermethylation phenotype, disrupt TET2 function, and impair hematopoietic differentiation. Cancer Cell. 2010;18(6):553-567.
7. Russler-Germain DA, Spencer DH, Young MA, et al. The R882H DNMT3A mutation associated with AML dominantly inhibits wild-type DNMT3A by blocking its ability to form active tetramers. Cancer Cell. 2014;25(4):442-454.
8. Glass JL, Hassane D, Wouters BJ, et al. Epigenetic identity in AML depends on disruption of nonpromoter regulatory elements and is affected by antagonistic effects of mutations in epigenetic modifiers. Cancer Discov. 2017;7(8):868-883.
9. Guryanova OA, Shank K, Spitzer B, et al. DNMT3A mutations promote anthracycline resistance in acute myeloid leukemia via impaired nucleosome remodeling. Nat Med. 2016;22(12):1488-1495.
10. Inoue S, Li WY, Tseng A, et al. Mutant IDH1 downregulates ATM and alters DNA repair and sensitivity to DNA damage independent of TET2. Cancer Cell. 2016;30(2):337-348.
11. Flavahan WA, Drier Y, Liau BB, et al. Insulator dysfunction and oncogene activation in IDH mutant gliomas. Nature. 2016;529(7584):110-114.
12. Cancer Genome Atlas Research Network, Ley TJ, Miller C, Ding L, et al. Genomic and epigenomic landscapes of adult de novo acute myeloid leukemia. N Engl J Med. 2013;368(22):2059-2074.
13. McCarthy DJ, Chen Y, Smyth. Differential expression analysis of multifactor RNA-seq experiments with respect to biological variation. Nucleic Acids Res. 2012;40(10):4288-4297.
14. Verhaak RG, Wouters BJ, Erpelinck CA, et al. Prediction of molecular subtypes in acute myeloid leukemia based on gene expression profiling. Haematologica. 2009;94(1):131-134.
15. Hothorn T, Lausen B. On the exact distribution of maximally selected rank statistics. Comput Stat Data An. 2003;43(2):121-137.